Structural and ELectrochemical Properties Of Layered $Na_x(NiCo)_yMn_{1-2y}O_2$ (X=0.5,0.8, 1.0) As Cathode Material For Sodium-Ion Batteries

K. Hemalatha,[1,2‡] M. Jayakumar,[1,3‡] and A. S. Prakash[1,2*]

[1]CSIR-CentralElectrochemicalResearchInstitute-Chennaiunit,CSIRMadrasComplex,Taramani, Chennai600113,India[2]AcademyofScientificandInnovativeResearch(AcSIR),CSIR-Central ElectrochemicalResearchInstitute-Chennaiunit,CSIRMadrasComplex,Chennai600113, India[3]Electroplating and Metal Finishing Division, CSIR-Central Electrochemical Research Institute, Karaikudi 630006, India

* Corresponding Author (prakash.as@gmail.com)

Abstract:

Scout for cost-effective energy storage devices and realization of high-performance electrode materialshasresultedincascadingintereston sodium-ion batteries.Inthepresentwork,theinfluenceofsodium stoichiometry and change in transition metal content on the structure and electrochemical performance of $Na_x(NiCo)_yMn_{1-2y}O_2$cathode is studied. Depending on the sodium stoichiometry and synthesis temperature, different phases such as O3, P3, and P2 type layered compounds were prepared by sol-gel method. The phase classification is based on the accommodation of Na ion in octahedral (O) or prismatic (P) environment and the numbers '2' or '3' specifies the number of metal oxide layers in a unit cell. The cycling profiles of O3, P3, and P2 phases were different although the redox peaks arising from the transition metals Ni, Co and Mn are same. Sodium insertion/de-insertion in O3-$Na_x(NiCo)_yMn_{1-2y}O_2$ were associated with several phase transitions comprisingbiphasicandmonophasicdomains.UnlikeO3phase,thecyclingpatternofP3andP2doesnot show multiple plateaus associated with several phase transitions. The phases O3, P3 and P2 could deliver discharge capacitiesintherange120to170mAh/gcorrespondingto0.5to0.7moles ofreversiblesodium.Allthephases of $Na_x(NiCo)_yMn_{1-2y}O_2$are air and moisture sensitive and long exposure to air results in a non-stoichiometric $Na_{x-a}(NiCo)_yMn_{1-2y}O_2 \cdot H_2O$ hydrated phase which greatly affects its electrochemical properties as the concentration of active sodium ionsdecreases.

Keywords: Na-ion batteries, energy storage, insertion electrodes, P2 and P3 phases, layered structure

1. Introduction

Lithium ion batteries have emerged front runners in meeting the energy needs of diverse devices ranging from handheld electronics to electric vehicles and this accomplishment is closely related to their high specific capacity and energy density[1-2]. However, high cost and limited resources of lithium compel researchers to look for alternate energy storage options. Such ventures are more attractive for niche applications such as electrical grid storage which need cost effective, safe and long life solutions while offering flexibility in terms of energy density. One such promising and viable option could be sodium ion batteries. Sodium demonstrates electrochemical properties and insertion mechanism similar to lithium and has widespread, abundant resources [3-4]. Although their research originated together with Li-ion batteries, Na-ion batteries have regained research interest in the recent years with the realization of Na insertion electrodes with capacities comparable with commercialized Li-ion cathodes [5].

Among various sodium compounds classified on the basis of their crystal structure, 2D sodium lamellar oxides of the generic formula Na_xMO_2 are widely investigated as cathode materials due to their structure and high specific capacity [6,7]. Na_xMO_2 compounds are composed of MO_2 layers with edge sharing MO_6 octahedra. Unary transition metal oxides such as Na_xMnO_2, Na_xCoO_2, Na_xNiO_2, $Na_xCrO_2$and Na_xVO_2depict complicated multiple potential plateaus driven by multi-structural transitions during cycling resultingin structural instability and continuous

capacity decay. A plausible approach could be doping certain metals such as Ni, Co, Mn, Ti, Al, Mg, Li which help in maintaining the structural integrity and improving the electrochemical performance by fine tuning the physical and chemical properties. For example, Ni doping increases the average potential through $Ni^{2+}/Ni^{3+}/Ni^{4+}$ redox that occurs above 3V. Mn doping contributes high specific capacity particularly at voltages below 2V. Co-substitution helps in the formation of passivation layer inhibiting capacity decay. Although ions such as Ti, Mg, Li and Al ions are electrochemically inert, they improve the structural stability. Considering these positive effects, optimal doping of such ions is likely to result in intercalation electrodes with enhanced structural stability and improved electrochemical performances. The resulting binary/ternary/quaternary/quinary oxides could be categorised into different polymorphs such as O3 (ABCABC), P3 (ABBCCA) and P2 (ABBA) based on the number of MO_2 layers in a unit cell (2, 3) and the occupancy of Na ion in octahedral (O) or prismatic (P) site. In general, P2 phases exhibit higher capacity and superior rate performance than O3 phases due to better structural stability and different Na-ion migration pathways [8]. By carefully altering sodium stoichiometry and dopants, it is possible to design compounds with varied structures and electrochemical performances.

With this background, the present work focuses on O-type and P-type phases of layered sodium transition metal oxides, $Na_x(NiCo)_yMn_{1-2y}O_2$ (x = 0.5, 0.8, 1.0) as cathode material for Na-ion batteries. Phase pure compositions synthesized by sol-gel method were characterized by XRD and SEM-EDS. Electrochemical performances as sodium intercalation cathode were studied and presented. For reasons of clarity, the results are discussed in context with our previous findings on O3-$NaNi_{0.33}Co_{0.33}Mn_{0.33}O_2$[9].

2. Experimental

2.l MaterialSynthesis

Layered $Na_x(NiCo)_yMn_{1-2y}O_2$(x=0.5, 0.8, 1) with chemical compositions; $Na_{0.5}Ni_{0.25}Co_{0.25}Mn_{0.5}O_2$, $Na_{0.8}Ni_{0.25}Co_{0.25}Mn_{0.5}O_2$, and $NaNi_{0.33}Co_{0.33}Mn_{0.33}O_2$, (hence forth referred as P2, P3 and O3, respectively) were prepared by the sol-gel method using acetates of Na, Ni, Co, Mn in the required stoichiometric ratio and citric acid as chelating agent. Sodium acetate fabout 5% excess was taken to compen sate the sodium loss that occurs at higher temperatures. The solution was made homogeneous and was heated on a hot plate at 80 °C to obtain a gel that upon further heating to 400 °C decomposed to yield an amorphous powder containing carbon residues. The decomposed product was heated in a muffle furnace at different temperatures (700 °C (P3) and 900 °C(O3 and P2)) for 12 h, then slowly cooled (1 °C/min) to 300 °C, removed from the furnace and transferred into an inert atmosphere glovebox where it was ground and stored to avoid any reaction with moisture and carbondioxide.P3 phase forms at lower temperature and P2 phase stabilizes at a higher temperature.

2.2 Material Characterization

Powder X-ray diffraction pattern (XRD) of the sample was recorded using Bruker D8 Advance Da Vinci diffractometer using CuKa radiation. The crystal structure and lattice parameters were analyzed by Rietveld refinement using the Fullprof program [10]. Scanning electron microscopy was performed using FESEM from Oxford instrument attached with EDS. The chemical composition of the sample was quantitatively estimated using Varian Spectra 220 atomic absorptions pectro photometer.

2.3 Electrochemical experiments

Electrochemical tests using organic electrolyte were carried out in Swage loktype cells assembledinan argon-filled glove box. The working electrodes were prepared by mixing 85 wt % of $Na_x(NiCo)_yMn_{1-2y}O_2$sample and 15 wt %of SP Carbon as conducting material. The sodium electrode was prepared by pressing a small piece of sodium metal onto a thin stainless disc. The electrolyte solution was 1 mol/L $NaPF_6$ dissolved in amixture of 1:1 volume percent of EC-PC. Aporous glass microfiber filter (What man) was used as a separator. The cell thus fabricated was cycled galvanostatically in the voltage range 1.5 V to 4.2 V versus sodium. Cyclic voltammetry experiments were carried out with IR compensation. All the electrochemical experiments were carried out at ambient temperature(303K) usingVMP-3Z Biologic multi-channel potentiostat/ galvanostat.

3. Results and Discussion

3.1 Crystal structure and Morphology analysis

The crystal structure of layered $Na_x(NiCo)_yMn_{1-2y}O_2$can be represented as alternate MO_2 slabs of edge shared MO_6 octahedra while Na^+lies in the interlayer spacing (Fig.1 and Fig. 2 insets). P3 and O3 phase show same type of Na atoms through hout the structure whereas P2 phase exhibits two types of Na atoms (edge shared and face shared)[8]. Powder X-ray diffraction pattern (XRD) of layered $Na_x(NiCo)_yMn_{1-2y}O_2$ indicated the absence of impurity phases. The XRD peaks corresponding to P2 phase could be indexed to a hexagonal system with $P6_3/mmc$ symmetry (No.194)(Fig.1). For O3 and P3 phases, the XRD pattern could be indexed with the rhombohedral symmetry (R-3m, No.166)(Fig. 2) [9]. The FESEM images of $Na_x(NiCo)_yMn_{1-2y}O_2$shows polyhedral shaped crystallites, mostly hexagonal in shape(Fig.1 and 2 insets). Nanoparticles in the range of 40- 90 nm were observed for P3 phase whereas, P2 phase displayed average particle size of 3mm. The particle size increases from nanometer to micronwith increase in synthesis temperature.

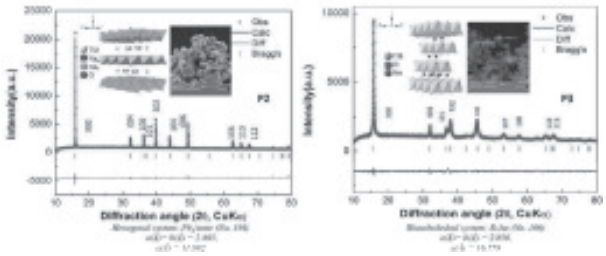


Figure 1. X-ray diffraction analysis and Full prof refinement of P2 and P3$Na_x(NiCo)_yMn_{1-2y}O_2$. Inset: Crystal structure and SEM micrographs of P2and P3phases.

3.2 Electrochemicalperformance

Cyclic voltammograms (CV) of P2and P3phases recorded at 0.1mV $s^{-1}$are presented in Fig. 2. CV portrays simpler and symmetric peaks in both phases representing the excellent reversibility of the electrode. three sharp oxidation peaks around 1.9, 3.3, and 3.6 V and their corresponding reduction peaks around 1.7, 3.25 and 3.55 V.The peaks below 2V represents Mn^{4+}/Mn^{3+} redox process and some of the Mn ions gets activated below 2V. The peaks around 3.3V and 3.6 V corresponds to $Ni^{3+}/Ni^{2+}$and Co^{4+}/Co^{3+}redox processes[4].

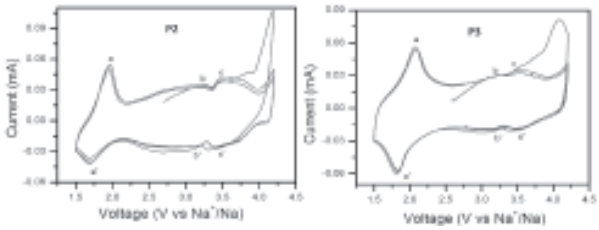


Figure2. Cyclic volt ammo grams of P2 and P3$Na_x(NiCo)_yMn_{1-2y}O_2$phases recorded at a scan rate of 0.1 mV/s.

Fig. 3 shows the galvnostatic charge-discharge cycling of P2and P3phases carried out in the voltage range 1.5 – 4.2 V at C/25 rate (insertion/de-insertion of 1 Na per formula unit in 25 h). The stair-like cycling profile of O3 phase indicates multiple potential plateaus associated with structural transitions[9]. Unlike O3 phase, the cycling profiles of P2 and P3 phases depict smooth cycling profiles devoid of multiple potential plateaus. The overlapping of the charge and discharge curves clearly demonstrates the excellent reversibility of the phases with minimum polarization and least structural change during sodiation/ desodiation. The P2 and P3 phases respectively deliverad is charge capacity of about 137and 180 mAh g^{-1} (Fig. 3 inset) corresponding to 0.75 and 0.57 moles of sodium. At C/10 rate, the capacity retention of P2and P3phases was about 87%and 91%, respectively. The O3 phase delivered a reversible capacity of about 120 mAh g^{-1} corresponding to 0.5 moles of reversible sodium without much irreversible loss even after 50 cycles [9]. Fig. 3b shows the rate performance of P2and P3phases. P2 phase delivered 140, 125,119, 100 and 89 mAh g^{-1} at C/10,C/5, C/2 and 1C rate, respectively. P3 phase shows reversible capacity of 150, 125, 100 and 77 $mAhg^{-1}$ at C/10, C/5, C/2 and 1C rate, respectively.

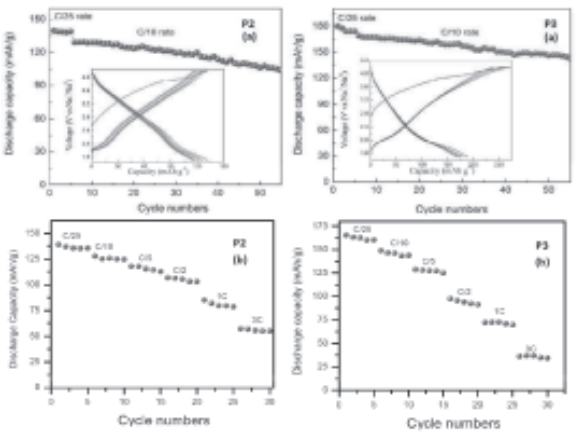


Figure3. Electrochemical performance of P2 and P3$Na_x(NiCo)_yMn_{1-2y}O_2$phases as Na-ion cathodes. (a) Capacity retention as a function of cycle number. Inset: Voltage versus capacity plot. (b) Rate performance of P2 and P3$Na_x(NiCo)_yMn_{1-2y}O_2$phases.

3.3 Moisture and air stability of$Na_x(NiCo)_yMn_{1-2y}O_2$

$$Na_x(NiCo)_yMn_{1-2y}O_2 + CO_2 + H_2O \rightarrow Na_{x-a}(NiCo)_yMn_{1-2y}O_2.H_2O + aNaOH + a/2Na_2CO_3 \quad (1)$$

The open circuit potential of P2, P3,and O3 phases vary between 2.8-2.4V which is below the reduction potential of water (3.94 V vs Na^+/Na). Hence, layered $Na_x(NiCo)_yMn_{1-2y}O_2$ phases react with moisture and carbondioxide forming sodium hydroxide and sodium carbonate, respectively(Eq.1). The refore the electrochemical performance of the resulting sodium deficient $Na_{x-a}(NiCo)_yMn_{1-2y}O_2$ or$Na_{x-a}(NiCo)_yMn_{1-2y}O_2.H_2O$ (hydrated phase) strongly affects its electrochemical properties as the concentration of active sodium ions decreases giving rise to structural transitions or increased interlayer spacing [8,9].While P3 structure loses its chemical stability on aging with water, P2 retains its hexagonal structure associated with incorporation of water molecules in the inter-layers(Fig.4).

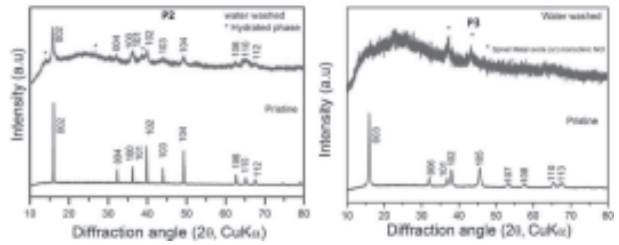


Figure4. Aqueous stability of P2 and P3 $Na_x(NiCo)_yMn_{1-2y}O_2$ phases.

4. Conclusions

Structure and electrochemical performances of $Na_x(NiCo)_yMn_{1-2y}O_2$(x = 0.5, 0.8, 1.0) cathode is studied as a function of sodium stoichiometry and transition metal content. X-ray analysis confirmed the formation of phase pure P2 and P3 $Na_x(NiCo)_yMn_{1-2y}O_2$withhexagonal and rhombohedra l symmetry, respectively. Electrochemical studies unveiled the strong relation between sodium content and performance;P3 phase with reversible 0.8 moles of Na delivered around 180 mAh/g with better capacity retention whereas P2 phase delivered 137 mAh/g corresponding to 0.55 moles of Na. Both P2 and P3 phases are sensitive to moisture which results in sodium loss and irreversible structural changes. The results disclose the significance of sodium and transition metal content in such phases to achieveNa-ion intercalation electrodes with superlative energy storage properties.

5. Acknowledgement

Ms. K. Hemalatha thanks Council of Scientific and Industrial Research (CSIR) for granting Senior Research Fellowship. This work was supported by Department of Science and Technology-Science and Engineering research board, New Delhi, under the grant scheme GAP 15/16.

6. References

1. J.M.TarasconandM.Armand, Nature, 2001, 414, 359-367.
2. M. Armand and J. M. Tarascon, Nature, 2008, 451, 652-657.
3. V. Palomares, M. C. Cabanas, E. C. Martinez, M. H. Han and T. Rojo, Energy Environ. Sci., 2013, 6,2312-2337.
4. D.Kundu, E.Talaie, V.Duffort and L.F.Nazar, Angew Chem. Int.Ed.,2015,54,2-20.
5. N.Yabuuchi, K.Kubota, M.Dahbi and S.Komaba, Chem.rev. 2014, 14, 11636-11682.
6. M. H. Han, E. Gonzalo, G. Singh and T. Rojo, Energy Environ. Sci., 2015,8, 81-102.
7. K.Kubota, N.Yabuuchi,H.Yoshida, M.Dahbi and S.Komaba, Mater.Res.Bull., 2014, 39, 416-.
8. C.Delmas, C.Fouassier and P.Hagenmuller, Physica B+C, 99, 1980, 81-85.
9. A. S. Prakash, M. Sathiya, K. Hemalatha, K. Ramesha, J.-M. Tarascon, Chem. Mater. 2012, 24, 1846– 1853
10. H. M. Rietveld, J. Appl.Crystallogr., 1969, 2, 65-71.